Published in final edited form as:
Neurotox Res. 2008 December ; 14(4): 367–382. doi:10.1007/BF03033861.

Unregulated Mitochondrial GSK3β Activity Results in NADH:Ubiquinone Oxidoreductase Deficiency

Taj D. King[a], **Buffie Clodfelder-Miller**[b], **Keri A. Barksdale**[c], and **Gautam N. Bijur**[a,*]

a*Department of Psychiatry and Behavioral Neurobiology, University of Alabama at Birmingham, Birmingham, AL 35294-0017.*

b*Comprehensive Neuroscience Center, University of Alabama at Birmingham, Birmingham, AL 35294-0017.*

c*Department of Neurobiology, University of Alabama at Birmingham, Birmingham, AL 35294-0017.*

Abstract

GSK3β is prominent for its role in apoptosis signaling and has been shown to be involved in Parkinson's disease (PD) pathogenesis. The overall effects of GSK3β activity on cell fate are well-established, but the effects of mitochondrial GSK3β activity on mitochondrial function and cell fate are unknown. Here we selectively expressed constitutively active GSK3β within the mitochondria and found that this enhanced the apoptosis signaling activated by the PD-mimetic NADH:ubiquinone oxidoreductase (complex I) inhibitors 1-methyl-4-phenylpyridinium ion (MPP^+) and rotenone. Additionally, expression of GSK3β in the mitochondria itself caused a significant decrease in complex I activity and ATP production. Increased mitochondrial GSK3β activity also increased reactive oxygen species production and perturbed the mitochondrial morphology. Conversely, chemical inhibitors of GSK3β inhibited MPP^+- and rotenone-induced apoptosis, and attenuated the mitochondrial GSK3β-mediated impairment in complex I. These results indicate that unregulated mitochondrial GSK3β activity can mimic some of the mitochondrial insufficiencies found in PD pathology.

Keywords

Glycogen synthase kinase-3β; Parkinson's disease; 1-Methyl-4-phenylpyridinium; Rotenone; Mitochondria; NADH:ubiquinone oxidoreductase; Complex I; Caspase-3; Reactive oxygen species; Apoptosis

INTRODUCTION

Glycogen synthase kinase-3ß (GSK3β) has emerged as a major therapeutic target due to its involvement in several neurodegenerative diseases, including Parkinson's disease (King *et al*., 2001; Chen *et al*., 2004; Jope and Johnson, 2004; Avraham *et al*., 2005; Chung *et al*., 2007; Wang *et al*., 2007; Yuan *et al*., 2008). GSK3β was originally discovered as a regulator of glycogen synthesis (Parker *et al*., 1982). However, GSK3β has also been shown to affect numerous cellular mechanisms including cell fate. GSK3β is typically constitutively active but phosphorylation at Ser-9 of GSK3β markedly attenuates its activity. In addition, GSK3β can be regulated by protein complex formation (Jope and Johnson, 2004), which is independent of phosphorylation at Ser-9.

*Corresponding author: Tel.: 1 (205) 996-2500; FAX: 1 (205) 934-2500; E-mail: E-mail: gautam@uab.edu.

GSK3β was initially thought to be localized in the cytosol (Hemmings *et al*., 1981). In fact, the largest pool of GSK3β does exist in the cytosol, but lesser amounts can be found in the nucleus (Diehl *et al*., 1998; Xavier *et al*., 2000; Bijur and Jope, 2001) and in the mitochondria (Bijur and Jope, 2003a,b; Hoshi *et al*., 2003). The existence of GSK3β in mitochondria suggests that it has access to substrates resident in this organelle, which could include proteins of the intrinsic apoptosis pathway sequestered in healthy mitochondria, as well as mitochondrial metabolic proteins. Numerous studies have listed the ramifications of unregulated GSK3β on cell fate, but to date the effects of unregulated mitochondrial GSK3β on the mitochondria and apoptosis signaling are largely unknown.

GSK3β is well known to play a role in apoptosis signaling. Unregulated GSK3β activity can activate apoptosis signaling on its own (Pap and Cooper, 1998), or enhance apoptosis by toxic stimuli that trigger mitochondrial-dependent apoptosis signaling. For example, GSK3β facilitates cell death induced by stressors such as heat shock (Bijur *et al*., 2000), osmotic stress (Rao *et al*., 2004), the generic apoptosis inducer staurosporine (Bijur *et al*., 2000), growth factor withdrawal (Hetman *et al*., 2000), mitochondrial toxins such as rotenone (King *et al*., 2001), endoplasmic reticulum toxins such as thapsigargin (Song *et al*., 2002), and genotoxic agents such as camptothecin (Watcharasit *et al*., 2002). Interestingly, both thapsigargin and camptothecin have been shown to increase GSK3β activity within the mitochondria (Song *et al*., 2002; Watcharasit *et al*., 2002). Conversely, inhibitors of GSK3β have been found to be neuroprotective. The classical GSK3β inhibitor lithium has been shown to provide protection against a host of physical and chemical stressors. Thus, an overall increase in GSK3β activity appears to enhance the lethality of various toxic stimuli by decreasing the ability of cells to mount a vigorous survival response.

Since many studies thus far have focused on outcomes related to overall increases in GSK3β activity, the goal of this study was to determine the ramifications of unregulated GSK3β activity within the confines of the mitochondria of SH-SY5Y neuroblastoma cells and to measure cellular responses to an increase in mitochondrial GSK3β activity. This report shows that increased mitochondrial GSK3β activity robustly inhibits NADH:ubiquinone oxidoreductase (complex I) activity, causes oxidative stress, potentiates caspase-3 activation by the Parkinson's disease-mimetic toxins 1-methyl-4-phenylpyridinium (MPP^+) and rotenone, and causes gross alterations in mitochondrial morphology.

METHODS

Materials

GSK3β inhibitor II was purchased from EMD Chemicals (Gibbstown, NJ) and all other chemicals were purchased from Sigma-Aldrich (St. Louis, MO) unless otherwise stated.

Plasmid Construction and Lentivirus Preparation

The constitutively active GSK3β (in which the Ser9 of GSK3β has been mutated to an Ala, S9A) fused to a mitochondrial localization sequence (MSVLTPLLLRGLTGSARRLPVPRAKIHSL) from subunit VIII of cytochrome oxidase pBIG2r construct (mS9AGSK3β) was a generous gift from Dr. Richard S. Jope (University of Alabama at Birmingham). The mitochondrial-targeted green fluorescent protein (pCMVMitoGFP or mGFP), which is used as a control in these studies, was purchased from Invitrogen (Carlsbad, CA). The pENTR Directional TOPO Cloning Kit (catalog number K2400-20) and the ViraPower Lentivirus Expression System (catalog numbers K4965-00 and K4967-00; Invitrogen) were used according to the manufacturer's instructions to package the plasmid constructs into lentivirus particles.

Production of S-inducible Cell Lines and Treatments

Human neuroblastoma SH-SY5Y cells were used to make stable cell lines that conditionally express mS9AGSK3β and mGFP in the presence of doxycycline, an analog of tetracycline. Briefly, wild-type SH-SY5Y cells were initially transduced with the tetracycline (Tet) repressor lentivirus (Lenti6/TR) construct using the Magnetofection-ViroMag R/L transduction kit (OZ Biosciences, Marseille, France) to enhance the efficiency of transduction for low viral titers. The cells were selected with 2 μg/ml blasticidin 24 h post-transduction and were allowed to grow for several days to allow time for the Tet repressor expression levels to increase. Subsequently, the Tet repressor stable cell lines were seeded (2.0×10^5 cells/plate) in 35 mm dishes and were transduced with the mS9AGSK3β (9.85×10^3) or mGFP (4.6×10^3) lentivirus constructs, using the Magnetofection-ViroMag R/L transduction kit, to establish stable-inducible cell lines for each of the constructs. The cell lines were grown in DMEM/F12 media (Cellgro, Herndon, VA) supplemented with 10% fetal bovine serum (Hyclone, Logan, UT), 2 mM L-glutamine, and 100 U/ml penicillin/100 μg/ml streptomycin. Cells were kept under selection with 50 μg/ml Zeocin and 2 μg/ml blasticidin until they were cultured for experimentation.

GSK3β Kinase Assay

Cells were lysed in immunoprecipitation (IP) lysis buffer (20 mM Tris, pH 7.5, 0.2% Nonidet P-40, 150 mM NaCl, 2 mM EDTA, 2 mM EGTA, 1 mM sodium orthovanadate, 100 μM phenylmethylsulfonyl fluoride, 10 μg/ml leupeptin, 10 μg/ml aprotinin, 5 μg/ml pepstatin, 1 nM okadaic acid, and 100 mM sodium fluoride). The lysates were sonicated in microcentrifuge tubes for 10s on ice and centrifuged at 20,800*g* for 15 min. After the protein concentration was determined by using the bicinchoninic acid method (Pierce, Rockford, IL), 100 μg of protein (1 μg/μl) was precleared with 60 μl of protein G-Sepharose beads for 3 h at 4°C then incubated with 2 μg of monoclonal GSK3β antibody (Pharmingen/Transduction Laboratories) for 3h at 4°C with gentle agitation. The immobilized immune complexes were washed three times with IP lysis buffer and three times with kinase assay buffer (20 mM Tris, pH 7.5, 5 mM $MgCl_2$, 1 mM dithiothreitol). Kinase activity was assayed in a total volume of 30 μl of kinase buffer containing 20 mM Tris, pH 7.5, 5 mM $MgCl_2$, 1 mM dithiothreitol, 250 μM ATP 1.4 μCi of [γ-^{32}P]ATP, and 100 μM phosphorglycogen synthase peptide-2 (YRRAAVPPSPSLSRHSSPHQSEDEEE) (Upstate Biotechnology, Inc., Lake Placid, NY). Glycogen synthase (Ala21) peptide-2 was used as a negative control. The samples were incubated at 30°C for 30 min, the reaction tubes were centrifuged for 1 min, and triplicate 9-μl aliquots of reaction supernatants were spotted onto 1 cm × 2 cm P81 filter paper. The filter papers were washed 4 times in 0.5% phosphoric acid for a total time of 1h, rinsed in 95% ethanol, air-dried, and counted in a liquid scintillation counter. The efficiency of GSK3β immunoprecipitation was determined by immunoblotting for GSK3β.

Immunofluorescence

Cells (mGFP and mS9AGSK3β) were cultured on poly-D-lysine-coated glass cover slips and subjected to treatments as indicated. The cells were treated with 1 nM MitoTracker (red-CMX-ROS, Invitrogen) for 1 h at 37°C, washed twice with warm phosphate buffered saline (PBS), then fixed and permeabilized with 2% paraformaldehyde for 20 min at 37°C and 0.1% triton-X 100 at room temperature for 5 min, respectively. The cover slips (mS9AGSK3β cells) were washed twice with PBS and incubated over-night at 4°C with mouse monoclonal anti-GSK-3ß antibody (1:250) diluted in PBS containing 5% bovine serum albumin (BSA). The cover slips were washed with PBS and incubated with anti-mouse Alexafluor green secondary antibody (1:4,000) in PBS containing 5% BSA for 1 h at room temperature. The cover slips were washed once with PBS, twice with deionized water, and were incubated with 0.2 μg/ml Hoechst 33342 at room temperature for 1 h. The cover slips were washed with deionized water, mounted onto

glass slides using Gel/Mount (Biomeda Corp., Foster City, CA), and examined by a fluorescent microscope (MicroBright Field, Inc.) set at 40x and 100× magnification.

Immunoblotting

Cells were washed twice with PBS and lysed in IP lysis buffer (20 mM Tris, pH 7.5, 150 mM NaCl, 2 mM EDTA, 2 mM EGTA, 1 mM sodium orthovanadate, 100 μM phenylmethylsulfonyl fluoride, 10 μg/ml leupeptin, 10 μg/ml aprotinin, 5 μg/ml pepstatin, 50 mM NaF, 1 nM okadaic acid, and 0.5% NP-40). The lysates were centrifuged at 20,817*g* for 10 min at 4°C and supernatants were collected. To obtain crude mitochondrial extracts, cells were washed with PBS, harvested in cavitation buffer (5 mM HEPES, pH 7.4, 3 mM $CaCl_2$, 1 mM EGTA, and 250 mM sucrose), and lysed by nitrogen cavitation (Bijur and Jope, 2003a). Lysed cells were centrifuged at 500*g* for 5 min, and the supernatant was centrifuged at 16,000*g* for 10 min. The membrane pellet was washed three times with cavitation buffer and lysed in IP lysis buffer. Protein concentrations were determined by using the bicinchoninic acid method. Cell lysates were mixed with Laemmli sample buffer (2% SDS) and placed in a boiling water for 5 min. Proteins (10 μg) were resolved in 7.5% SDS-polyacrylamide gels, and transferred to nitrocellulose. Blots were probed with antibodies to total GSK3β (BD Transduction Laboratories, Lexington, KY), PARP (Cell Signaling Technologies, Beverly, MA), and V5-tag (Invitrogen, Carlsbad, CA). Immunoblots were developed using horseradish peroxidase-conjugated goat anti-mouse or goat anti-rabbit IgG (Bio-Rad Laboraories, Hercules, CA), followed by detection with enhanced chemiluminescence. Immunoblots were quantitated by scanning densitometry using UN-SCAN-IT image digitizing software (Silk Scientific Inc., Orem, Utah).

Transmission Electron Microscopy

Cells from each sample were collected and fixed with Karnovsky's fixative (2% paraformaldehyde/ 2.55 glutaraldehyde in 0.1 M sodium cacodylate buffer). Subsequently, the samples were rinsed several times with Karnovsky's buffer followed by post fixation with 1% osmium tetroxide for 1 h. The samples were rinsed with PBS for 1 h and were dehydrated through a series of graded ethyl alcohols from 50% to 100%. After dehydration the samples were infiltrated with two changes of 100% propylene oxide for 10 minutes each and a 50:50 mixture of propylene oxide and the embedding resin (Embed 812, Electron Microscopy Sciences, Fort Washington, PA) for 12–18 h. The samples were then transferred to fresh 100% embedding media twice for at least 1 h. The tissue was then embedded in a fresh change of 100% embedding media. Following 12–18 h in the oven at 60°C for polymerization, the blocks were then ready to section. The resin blocks were sectioned at 1–2 microns with a diamond histo knife using an ultramicrotome and stained with Toluidine Blue. These sections were used as a reference to trim blocks for thin sectioning. The appropriate blocks were then thin sectioned using a diamond knife (Diatome, Electron Microscopy Sciences) at 70–100 nm and sections were placed on either copper or nickel mesh grids. The sections were stained with uranyl acetate and lead citrate for contrast. The grids were then viewed on a FEI Tecnai Twin 120kv transmission electron microscope (FEI, Hillsboro, OR). Digital images were taken with an AMT CCD camera, and stored on a memory storage device. Images were analyzed and quantitated by Image J. Briefly, 48 to 62 mitochondria per grid were randomly circumscribed and the area was quantitated for each mitochondrion.

Complex I Activity Assay

Complex I activity was determined by measuring the rate of NADH oxidation at 340 nm using ubiquinone-2 as the electron acceptor. The rate sensitivity to rotenone (10 μM) was taken to be complex I activity (Milakovic *et al*., 2005). Crude mitochondrial extracts were used to measure complex I activity. Briefly, cells were washed with phosphate buffered saline,

harvested in cavitation buffer (5 mM HEPES, PH 7.4, 3 mM $CaCl_2$, 1 mM EGTA, and 250 mM sucrose), and lysed by nitrogen cavitation. Lysed cells were centrifuged at 700*g* for 5 min, and the supernatant was centrifuged at 16,000*g* for 10 min. The membrane pellet was washed three times with cavitation buffer and freeze-thawed three times (at −80°C) in cavitation buffer. Then the pellet was centrifuged at 16,000*g* for 5 min and was resuspended in 1 ml ddH_2O. The pellet suspension was centrifuged at 16,000*g* for 5 min and resuspended in cavitation buffer. The pellet suspension was sonicated on ice three times at 10 second intervals. Protein concentration was determined by the bicinchoninic method and standardized (50 μg) for the complex I assay.

ATP Production Assay

Mitochondria were isolated in cavitation buffer (5 mM HEPES pH 7.4, 3 mM $MgCl_2$, 1 mM EGTA, 250 mM Sucrose) using nitrogen cavitation and centrifugation. Protein concentrations were determined prior to the assay using the bicinchoninic acid assay (Pierce). Mitochondrial protein (250 μg) was used for each reaction, and the mitochondria were spun down, re-suspended in cavitation buffer, and were pelleted on ice until ready for use. For the ATP production assay, pellets were re-suspended in 190 μl respiration buffer (20 mM HEPES-KOH pH 7.4, 80 mM KOAc, 5 mM $MgOAc_2$, 250 mM sucrose, 1 mM pyruvate, 1 mM malate, or 5 mM succinate. Buffer B (0.5 M Tris-Acetate pH 7.75, 0.8 mM D-Luciferin, 20 μg/ml luciferase) (10 μl) was immediately added to the reaction, and sample luminescence was read in standard mode on a Turner 20/20 luminometer for 4 seconds with no delay. ADP was added to the sample at a final concentration of 0.1 mM, and the luminescence was read every 4 seconds for 160–180 seconds.

ROS Measurement

To measure intracellular production of ROS, cells were placed in Kreb's buffer (30 mM HEPES pH 7.4, 122 mM, 4.9 mM KCl, 1.2 mM $MgSO_4$, 1.2 mM KH_2PO_4, 1.3 mM $CaCl_2$, 3.6 mM $NaHCO_3$, and 11 mM glucose) and treated with 100 μM 2,7-dichlorofluorescein diacetate (Molecular Probes, Eugene, OR) for 30 min at 37°C. Cells were washed twice with Kreb's buffer and sonicated in a buffer containing 50 mM KH_2PO_4, 0.1 mM EDTA, and 0.1% 3-[(3-cholamidopropyl)-dimethylammonio]-1-propane-sulfonate (pH 7.0). The mixture was centrifuged at 2000*g* for 10 min at 4°C. The supernatant was used to determine intracellular oxidant production by monitoring its florescence on a Bio-Tek Synergy fluorescence spectrophotometer at 485 nm excitation and 528 nm emission.

RESULTS

Overexpression of GSK3β in the Mitochondria

Previously it was shown that global overexpression of GSK3β in SH-SY5Y cells facilitates apoptosis by a variety of toxic stimuli. The goal was to examine how selectively increasing GSK3β activity in the mitochondria would affect apoptosis signaling. GSK3β expression was increased specifically within the confines of the mitochondria of SH-SY5Y cells. Stable cell lines were produced by lentivirus-mediated gene transduction of a tetracycline (doxycycline)-inducible, constitutively active mutant of GSK3β, in which the regulatory Ser9 site was mutated to an Ala. A mitochondrial targeting sequence from subunit VIII of cytochrome oxidase, a mitochondrial inner membrane protein (Rizzuto *et al*., 1992), was added at the *N*-terminus of the protein (mS9AGSK3β). The initial goal was to test if the mitochondrial targeting sequence would direct the expressed proteins specifically to the mitochondria. Green fluorescent protein fused to the mitochondrial targeting sequence (mGFP) and mS9AGSK3β were transduced into cells by lentivirus (FIG. 1A). Cells stably expressing mGFP and mS9AGSK3β were stained with Mito Tracker (red-CMX-ROS, Invitrogen), which causes actively respiring mitochondria to fluoresce red. The image in FIG. 1A (top panel) shows complete co-localization (yellow)

of the mGFP autofluorescence (green) with the Mito Tracker (red). Similarly, expression of the V5-tagged mS9AGSK3β, using the V5 anti-body for immunofluorescence staining, was also found to be completely co-localized with Mito Tracker (FIG. 1A, lower panel), verifying that both the expressed proteins are selectively localized to the mitochondria. The nuclei (Hoechst 33342, blue) are devoid of any staining of the expressed mitochondrial proteins. To examine the extent of mS9AGSK3β protein expression, a dose response and time course of doxycycline (Dox) treatment were performed, and whole cell lysates were immunoblotted for total GSK3β and for the V5 C-terminal tag on the expressed mS9AGSK3β. Robust expression of mS9AGSK3β commenced with as little as 0.05 μg/ml Dox and reached maximum expression following the addition of 0.1 μg/ml Dox (FIG. 1B). Treatment of cells with 1 μg/ml Dox increased the expression of mS9AGSK3β time-dependently, with mS9AGSK3β reaching maximum expression by 24 h and remaining at this level beyond 48 h following Dox treatment. The total increase in GSK3β protein levels (endogenous GSK3β plus mS9AGSK3β) was 160% over control. There was essentially no expression of mS9AGSK3β in the absence of Dox indicating that the expression is tightly regulated. To further confirm that mS9AGSK3β was localized to the mitochondria and that there was no "leakage" of protein into the cytosol, cells treated without and with Dox were fractionated into cytosolic and mitochondrial fractions and immunoblotted with V5 antibody to detect mS9AGSK3β (FIG. 1C). The expression of mS9AGSK3β was evident almost entirely in the mitochondrial fraction. An extended exposure of the immunoblot film did reveal a very minute amount of mS9AGSK3β in the cytosolic fraction, which could be newly synthesized protein destined for the mitochondria. To verify that mS9AGSK3β is constitutively active and to test the increase in GSK3β activity in Dox+ cells compared to the control Dox− cells, cells were induced with doxycycline for 24 h. Whole cell lysates were used to measure the overall increase in GSK3β activity as described in "Methods". The total GSK3β activity increased significantly by 162% (FIG. 1D) indicating that mS9AGSK3β is constitutively catalytically active.

Unregulated mitochondrial GSK3β activity facilitates apoptosis induced by mitochondrial complex I inhibition

Previously, global expression of GSK3β was shown to enhance caspase-3 activity and apoptosis induced by mitochondrial complex I inhibitors (King *et al*., 2001), endoplasmic reticulum stress (Song *et al*., 2002), genotoxic stress (Watcharasit *et al*., 2002), and staurosporine and heat shock (Bijur *et al*., 2000). The goal was to test if unregulated GSK3β activity sequestered in the mitochondria would have similar affects on apoptosis signaling. Expression of mS9AGSK3β was induced by Dox treatment (1 μg/ml) for 24 h. mS9AGSK3β expression alone did not cause any cell toxicity and no caspase-3 activity could be detected (FIG. 2A). The control, non-induced (Dox−) cells, and the induced, mS9AGSK3β-expressing (Dox+) cells were treated with 5 mM MPP^+, 5 μM rotenone, 2 μM thapsigargin, and 1 μM camptothecin for 4 h. The caspase-3-dependent cleavage of the 116-kDa poly (ADP-ribose) polymerase (PARP) to the 85-kDa fragment during apoptosis (Tewari *et al*., 1995; Oliver *et al*., 1998) was measured by immunoblot analysis. Induction of mS9AGSK3β expression significantly augmented (FIG. 2A) MPP^+- and rotenone-induced caspase-3 activities (FIG. 2A), 264% and 395% of control. However, mS9AGSK3β expression did not potentiate caspase-3 activity induced by treatments with thapsigargin, an endoplasmic reticulum toxin, or camptothecin, a genotoxic agent. Caspase-3 activity was also induced by the complex II inhibitor 3-nitropropionic acid (3-NP) (Ludolph *et al*., 1992) (20 mM for 24 h), but mS9AGSK3β expression failed to cause any facilitation of 3-NP-induced apoptosis. Treatment of cells with staurosporine and heat shock also activated caspase-3, but mS9AGSK3β expression did not enhance caspase-3 activation by these general apoptosis inducers (data not shown). Expression of GFP in the mitochondria (mGFP) had no effects on MPP^+ and rotenone-induced caspase-3 activity (FIG. 2B). To confirm that the facilitation of MPP^+-and rotenone-induced apoptosis was due to increased GSK3β activity, cells were treated

with two chemically different GSK3β inhibitors, 2-thio(3-iodobenzyl)-5-(pyridyl)-[1,3,4]-oxadiazole, also known as GSK3β inhibitor II (Naerum, *et al*., 2002), and lithium (Klein and Melton, 1996) to determine if facilitation of caspase-3 activity could be blocked. Treatment of cells with GSK3β inhibitor II (5 μM) 30 min prior to MPP^+ and rotenone treatments inhibited caspase-3 activity (FIG. 2C) and blocked the mS9AGSK3β-mediated enhancement of caspase-3 activity. Similarly, acute treatment of cells with lithium (20 mM) completely blocked the mS9AGSK3β-mediated facilitation of MPP^+ and rotenone-induced caspase-3 activity (FIG. 2D). The blockade of caspase-3 activity by the GSK3β inhibitors indicates that increased GSK3β activity in the mitochondria enhances the toxicity of the complex I inhibitors. The augmentation of caspase-3 activity specifically by the complex I inhibitors, implies that GSK3β signaling converges on complex I.

Unregulated mitochondrial GSK3β inhibits complex I activity

Given the fact that expression of mS9AGSK3β enhanced apoptosis induced by two different complex I inhibitors, but not other apoptosis inducers, we theorized that the deleterious effects of increased mitochondrial GSK3β may be mediated through a defect in complex I activity. Therefore, complex I activity was measured in mS9AGSK3β induced and non-induced cells. As hypothesized, complex I activity was found to be significantly attenuated by 70% in mS9AGSK3β-expressing cells compared to the noninduced cells (Table I). Treatment of mS9AGSK3β-expressing cells with GSK3β inhibitor II reversed the repression of complex I activity. Lithium was also used to inhibit mS9AGSK3β activity; however, lithium was added directly to the mitochondrial lysates because lithium reversibly binds to the magnesium binding site of GSK3β, and the mitochondrial isolation process can easily disrupt the binding of lithium to GSK3β and reactivate the enzyme. The addition of lithium also significantly reversed GSK3β-mediated complex I inhibition (Table I). Treatment with the GSK3β inhibitors alone in the non-induced control cells had no effects on complex I activity. Complex I activity was measured in the mGFP cells to further control for artifacts of increased protein expression. There was no significant difference in complex I activity in the mGFP induced cells compared to that of the non-induced cells (Table I). Since the entry point of electrons from NADH is complex I, and a disruption of complex I should theoretically decrease energy production, mitochondrial ATP production was measured. ATP production by mitochondria from mS9AGSK3β-expressing cells decreased in parallel with the decreased complex I activity (FIG. 3). GSK3β inhibitor II treatment of induced cells partially restored mitochondrial ATP production. Curiously, GSK3β inhibitor II treatment of non-induced cells caused a slight attenuation of ATP synthesis. Together this data shows that unregulated mitochondrial GSK3β severely impairs complex I activity and prevents normal mitochondrial ATP production.

Unregulated mitochondrial GSK3β activity induces reactive oxygen species (ROS) production

Complex I dysfunction has been shown to increase the generation of ROS (Hasegawa *et al*., 1990; Cleeter *et al*., 1992; Gonzalez-Polo *et al*., 2003). To test if increased mitochondrial GSK3β activity also elevates intracellular ROS production, mS9AGSK3β expression was induced with Dox for 24 h and ROS production was measured. There was a significant increase in intracellular ROS production (137 ± 8%) in the mS9AGSK3β-expressing cells compared to the non-induced cells (FIG. 4A), and post-induction treatment with GSK3β inhibitor II completely blocked mS9AGSK3β-mediated ROS production (FIG. 4A). Furthermore, treatment with lithium also significantly reduced the levels of intracellular ROS in mS9AGSK3β-expressing cells (FIG. 4B). Treatment of the non-induced control cells with the GSK3β inhibitors did not markedly affect ROS levels. As another control, SH-SY5Y cells that constitutively express the tetracycline repressor were also treated with doxycycline. There was

no significant increase in ROS production following Dox treatment of control cells, indicating that Dox treatment alone did not affect intracellular ROS production (FIG. 4C).

Increased mitochondrial GSK3β activity alters mitochondrial morphology

Aberrant mitochondrial function, including complex I deficiency and elevations in intracellular ROS production can affect mitochondrial morphology (Koopman *et al*., 2008) and cause mitochondrial fission. Therefore, to test if increased expression of mS9AGSK3β alters mitochondrial morphology, mS9AGSK3β cells were treated with Dox, stained with Mito Tracker, and immunofluorescently labeled with GSK3β antibody. The diffuse green staining is endogenous GSK3β, but the expressed mS9AGSK3β which appears punctuate colocalizes with the Mito Tracker (FIG. 5A). Interestingly, the mitochondria themselves appear fragmented in the mS9AGSK3β-expressing cells. Upon closer observation the mitochondria in the control mGFP-expressing cells and the non-induced mS9AGSK3β cells appear fibrous (FIG. 5B). By contrast, in cells expressing mS9AGSK3β, the mitochondria appear fragmented and punctiform (FIG. 5B). Post-induction treatment of the mS9AGSK3β cells with GSK3β inhibitor II partially restored the mitochondrial morphology (FIG. 5B) although some fragmented mitochondria were still evident.

To more closely visualize mitochondrial morphology, the mitochondria were viewed by transmission electron microscopy. Normal mitochondria in control cells displayed classical morphological features, including an elongated shape with well-defined cristae, as seen in the mGFP-expressing cells and the mS9AGSK3β noninduced cells (FIG. 5C). However, the morphology of the mitochondria appeared smaller in size in cells expressing mS9AGSK3β. Moreover, the cristae appeared more de-convoluted and vacuole-like in the mS9AGSK3β-expressing cells compared to the non-induced cells (FIG. 5D). To test if inhibition of mS9AGSK3β rectifies the aberrant mitochondrial morphology, mS9AGSK3β expression was induced for 24 h followed by post-induction treatment with GSK3β inhibitor II or lithium. Treatment of cells with GSK3β inhibitor II or lithium (data not shown) reversed the affects of mS9AGSK3β expression on mitochondrial morphology (FIG. 5C), as they resembled mitochondria in the control cells. Area quantitation revealed that the size of mitochondria in the mS9AGSK3β-expressing cells was significantly (50%) smaller than the mitochondria in the mS9AGSK3β non-induced cells (FIG. 5E). Treatment of the mS9AGSK3β-expressing cells with GSK3β inhibitor II or with lithium either partially or completely, respectively restored the mitochondria to their original size (FIG. 5E). There were no significant differences in mitochondrial size in the mGFP-expressing cells and the mS9AGSK3β non-induced cells (FIG. 5E). Thus, unregulated GSK3β activity can affect gross mitochondrial morphology.

DISCUSSION

GSK3β is typically viewed as one continuous intracellular pool, but in reality endogenous GSK3β exists within different subcellular compartments, including the mitochondria (Bijur and Jope, 2003a; Hoshi *et al*., 2003), and it has previously been shown that this fraction of GSK3β is highly activated relative to GSK3β in the cytosol (Bijur and Jope, 2003b). However, almost nothing is known about how GSK3β signaling emanating from within the mitochondria affects this organelle. The key finding in this study is that expression of constitutively active GSK3β inside the mitochondria robustly inhibits complex I function.

It is now well established that unregulated GSK3β augments apoptosis signaling. Our initial goal was to determine if increased GSK3β activity within the confines of the mitochondria would have similar affects on apoptosis. However, expression of mS9AGSK3β alone did not activate caspase-3, but it did facilitate apoptosis induced by two apoptosis inducers known to be influenced by GSK3β over-expression, MPP^+ and rotenone. A variety of apoptosis inducers were tested; including thapsigargin, an endoplasmic reticulum toxin, and camptothecin, a

genotoxic agent, as well as the general apoptosis inducers heat shock and staurosporine (data not shown), none of which were affected by mS9AGSK3β expression. However, caspase-3 activation by two chemically unrelated complex I inhibitors, MPP^+ and rotenone, was significantly enhanced by mS9AGSK3β expression. Interestingly, untargeted overexpression of GSK3β has been shown to enhance apoptosis by all of these treatments (Bijur *et al*., 2000; King *et al*., 2001; Song *et al*., 2002; Watcharasit *et al*., 2002), but overexpression of GSK3β in the mitochondria selectively potentiated caspase-3 activity induced by the complex I inhibitors. To test if mS9AGSK3β was simply enhancing the toxicity of mitochondrial toxins, cells were treated with the complex II inhibitor 3-NP. However, 3-NP-induced caspase-3 activity was also unaffected by mS9AGSK3β expression, which indicates that unregulated mitochondrial GSK3β activity selectively exacerbates the effects of complex I inhibition. On the basis of this result it was theorized that GSK3β might be affecting complex I function and bolstering the toxicity of the complex I inhibitors.

Complex I, (NADH:ubiquinone oxidoreductase, EC 1.6.5.3), is the point of entry for electrons destined for the electron transport chain from NADH. It is also the least understood and the largest protein component of the electron transport chain. Measurement of complex I activity from isolated mitochondria revealed that expression of the mS9AGSK3β significantly reduces complex I function and this decrease in activity could be reversed by the GSK3β inhibitors GSK3β inhibitor II and lithium. However, GSK3β inhibitor treatments alone did not increase basal complex I activity, indicating that normal endogenous GSK3β activity does not suppress complex I. Recently, it was shown that MPP^+ and rotenone treatments increase overall GSK3β activity (Wang *et al*., 2007; Chen *et al*., 2008). In addition, a previous report by our group (King *et al*., 2001) showed that inhibition of the upstream phosphatidylinositol 3-kinase/Akt signaling pathway, which is known to activate GSK3β, and untargeted overexpression of GSK3β facilitated MPP^+ and rotenone-induced apoptosis. However, none of these studies identified the different intracellular pools of GSK3β that are activated. Nevertheless, it is conceivable that increased GSK3β activity could contribute to the inhibition of complex I by MPP^+ and rotenone and partially contribute to their apoptosis-inducing effects. Normal complex I function maintains the proton gradient across the inner mitochondrial membrane which is required for ATP production. ATP synthesis was noticeably decreased by isolated mitochondria from mS9AGSK3β-expressing cells compared to control cells, which could be partially reversed by GSK3β inhibitor II treatment. Since complex I is the first point of entry for electrons it therefore makes sense that disabling complex I function by unregulated mitochondrial GSK3β activity would markedly affect mitochondrial energy production. Thus, this is the first report showing unregulated GSK3β as a potent complex I inhibitor; however, the exact mechanisms by which GSK3β inhibits complex I remain to be elucidated.

Complex I is known to be one of two major sources of ROS in the electron transport chain, the other being complex III (Camello-Almarez *et al*., 2006; Grivennikova and Vinogradov, 2006). Complex I inhibitors including MPP^+ and rotenone have previously been shown to increase ROS production (Hasegawa *et al*., 1990; Cleeter *et al*., 1992; Gonzalez-Polo *et al*., 2003). Since increased mitochondrial GSK3β activity impairs complex I function we hypothesized that unregulated mito-chondrial GSK3β activity would also enhance ROS production. In fact, increased expression of mS9AGSK3β facilitated the production of ROS and inhibition of mitochondrial GSK3β with GSK3β inhibitor II and lithium completely blocked GSK3β-mediated ROS production.

The most visible sign that unregulated GSK3β affects mitochondria was the morphological changes of Mito Tracker-stained mitochondria and the observable decrease in the size of mitochondria in mS9AGSK3β-expressing cells. Since increased mitochondrial GSK3β activity bolstered ROS production, it is likely that ROS triggers mitochondrial fission. In a recent study, ROS levels were discovered to be higher in cells with fragmented mitochondria (Koopman *et*

al., 2008). Also, in that same study, Hela cells were transfected with dynamin-related protein-1, an important mediator in mitochondrial fission, which induced mitochondrial fragmentation but not ROS production; thus, suggesting that ROS may act upstream of mitochondrial fission. Although it is not known how ROS may facilitate mitochondrial fission, it is thought that increases in intracellular ROS levels may regulate the expression and/or recruitment of mitochondrial fission/fusion proteins (Koopman *et al*., 2008). Therefore, the abundance of fragmented mitochondria in the mS9AGSK3β-induced cells but not in the mS9AGSK3β-non-induced cells or the mGFP-induced cells may be a result of increased GSK3β-mediated ROS production. The facilitation of MPP^+- or rotenone-induced apoptosis by mS9AGSK3β may be due in part to an increase in mitochondrial fission caused by GSK3β-mediated inhibition of complex I. Mitochondrial fission under normal conditions does not necessarily elicit the activation of downstream effector caspases (reviewed in Bossy-Wetzel *et al*., 2003); however, increased mitochondrial fission may sensitize the cells to certain apoptosis inducers including MPP^+ and rotenone. Therefore, an increase in mitochondrial GSK3β activity may serve to prime mitochondria for the release of pro-apoptotic factors (*i.e.*, AIF, cytochrome c) from the mitochondria upon stimulation with complex I inhibitors.

The findings in this report are particularly interesting from the standpoint that complex I dysfunction has been intrinsically linked most notably to Parkinson's disease (Parker *et al*., 1989; 2008; Swerdlow *et al*., 1996; Gu *et al*., 1998). Abnormal mitochondrial morphology, which may be indicative of excessive mitochondrial fission, has also been linked to neurodegenerative diseases, including Parkinson's disease (Trimmer *et al*., 2000). MPP^+ and rotenone are well known Parkinson's disease-mimetic toxins that cause selective apoptosis of dopaminergic neurons (Javitch *et al*., 1985; Betarbet *et al*., 2000) and motor deficits in animal models mirroring the palsy seen in this neurodegenerative disease. There is also growing evidence of GSK3β's involvement in Parkinson's disease (King *et al*., 2001; Chen *et al*., 2004; Avraham *et al*., 2005; Chung *et al*., 2007; Wang *et al*., 2007; Yuan *et al*., 2008). The present report illustrates that unregulated GSK3β in the mitochondria inhibits complex I activity, one of the major hallmarks of Parkinson's disease pathophysiology, the sequelae of which includes oxidative stress, decreased ATP production, and mitochondrial fission. Taken together, these studies raise the possibility that mitochondrial GSK3β could be a potential target for Parkinson's disease treatment.

Abbreviations

Dox, doxycycline; GSK3β, glycogen synthase kinase-3ß; mGFP, mitochondrial-targeted green fluorescent protein; mS9AGSK3β, mitochondrial-targeted constitutively active GSK3β; MPP^+, 1-methyl-4-phenylpyridinium; 3-NP, 3-nitroproprionic acid; ROS, reactive oxygen species.

Acknowledgements

This work was supported by NIH grant NS044853, the NIH Alabama Neuroscience Blueprint Core Grant NS57098, and the UAB Neuroscience Core NS47466.

References

Avraham E, Szargel R, Eyal A, Rott R, Engelender S. Glycogen synthase kinase 3β modulates synphilin-1 ubiquitylation and cellular inclusion formation by SIAH: implications for proteasomal function and Lewy body formation. J. Biol. Chem 2005;280:42877–42886. [PubMed: 16174773]

Betarbet R, Sherer TB, MacKenzie G, Garcia-Osuna M, Panov AV, Greenamyre JT. Chronic systemic pesticide exposure reproduces features of Parkinson's disease. Nat. Neurosci 2000;3:1301–1306. [PubMed: 11100151]

Bijur GN, Jope RS. Proapoptotic stimuli induce nuclear accumulation of glycogen synthase kinase-3β. J. Biol. Chem 2001;276:37436–37442. [PubMed: 11495916]

Bijur GN, Jope RS. Rapid accumulation of Akt in mitochondria following phosphatidylinositol 3-kinase activation. J. Neurochem 2003a;87:1427–1435. [PubMed: 14713298]

Bijur GN, Jope RS. Glycogen synthase kinase-3β is highly activated in nuclei and mitochondria. Neuroreport 2003b;14:2415–2419. [PubMed: 14663202]

Bijur GN, De Sarno P, Jope RS. Glycogen synthase kinase-3β facilitates staurosporine- and heat shock-induced apoptosis. Protection by lithium. J. Biol. Chem 2000;275:7583–7590. [PubMed: 10713065]

Bossy-Wetzel E, Barsoum MJ, Godzik A, Schwarzenbacher R, Lipton SA. Mitochondrial fission in apoptosis, neurodegeneration and aging. Curr. Opin. Cell. Biol 2003;15:706–716. [PubMed: 14644195]

Camello-Almaraz C, Gomez-Pinilla PJ, Pozo MJ, Camello PJ. Mitochondrial reactive oxygen species and Ca^{2+} signaling. Am. J. Physiol. Cell. Physiol 2006;291:1082–1088.

Chen G, Bower KA, Ma C, Fang S, Thiele CJ, Luo J. Glycogen synthase kinase 3β (GSK3β) mediates 6-hydroxydopamine-induced neuronal death. FASEB J 2004;18:1162–1164. [PubMed: 15132987]

Chen YY, Chen G, Fan Z, Luo J, Ke ZJ. GSK3β and endoplasmic reticulum stress mediate rotenone-induced death of SK-N-MC neuroblastoma cells. Biochem. Pharmacol 2008;76:128–138. [PubMed: 18508033]

Chung CY, Koprich JB, Endo S, Isacson O. An endogenous serine/threonine protein phosphatase inhibitor, G-substrate, reduces vulnerability in models of Parkinson's disease. J. Neurosci 2007;27:8314–8323. [PubMed: 17670978]

Cleeter MW, Cooper JM, Schapira AH. Reversible inhibition of mitochondrial complex I by 1-methyl-4-phenylpyridinium: evidence for free radical involvement. J. Neurochem 1992;58:786–789. [PubMed: 1729421]

Diehl JA, Cheng M, Roussel MF, Sherr CJ. Glycogen synthase kinase-3β regulates cyclin D1 proteolysis and sub-cellular localization. Genes Dev 1998;12:3499–34511. [PubMed: 9832503]

González-Polo RA, Soler G, Alvarez A, Fabregat I, Fuentes JM. Vitamin E blocks early events induced by 1-methyl-4-phenylpyridinium (MPP+) in cerebellar granule cells. J. Neurochem 2003;84:305–315. [PubMed: 12558993]

Grivennikova VG, Vinogradov AD. Generation of superoxide by the mitochondrial Complex I. Biochim. Biophys. Acta 2006;1757:553–561. [PubMed: 16678117]

Gu M, Cooper JM, Taanman JW, Schapira AH. Mitochondrial DNA transmission of the mitochondrial defect in Parkinson's disease. Ann. Neurol 1998;44:177–186. [PubMed: 9708539]

Hasegawa E, Takeshige K, Oishi T, Murai Y, Minakami S. 1-Methyl-4-phenylpyridinium (MPP+) induces NADH-dependent superoxide formation and enhances NADH-dependent lipid peroxidation in bovine heart submitochondrial particles. Biochem. Biophys. Res. Commun 1990;170:1049–1055. [PubMed: 2167668]

Hemmings BA, Yellowlees D, Kernohan JC, Cohen P. Purification of glycogen synthase kinase 3 from rabbit skeletal muscle. Copurification with the activating factor (FA) of the (Mg-ATP) dependent protein phosphatase. Eur. J. Biochem 1981;119:443–451. [PubMed: 6273157]

Hetman M, Cavanaugh JE, Kimelman D, Xia Z. Role of glycogen synthase kinase-3β in neuronal apoptosis induced by trophic withdrawal. J. Neurosci 2000;20:2567–2574. [PubMed: 10729337]

Hoshi M, Sato M, Kondo S, Takashima A, Noguchi K, Takahashi M, Ishiguro K, Imahori K. Different localization of tau protein kinase I/glycogen synthase kinase-3β from glycogen synthase kinase-3αa in cerebellum mitochondria. J. Biochem 2003;118:683–685. [PubMed: 8576078]

Javitch JA, D'Amato RJ, Strittmatter SM, Snyder SH. Parkinsonism-inducing neurotoxin, *N*-methyl-4-phenyl-1,2,3,6 tetrahydropyridine: uptake of the metabolite *N*-methyl-4-phenylpyridine by dopamine neurons explains selective toxicity. Proc. Natl. Acad. Sci. USA 1985;82:2173–2177. [PubMed: 3872460]

Jope RS, Johnson GV. The glamour and gloom of glycogen synthase kinase-3. Trends Biochem. Sci 2004;29:95–102. [PubMed: 15102436]

King TD, Bijur GN, Jope RS. Caspase-3 activation induced by inhibition of mitochondrial complex I is facilitated by glycogen synthase kinase-3ß and attenuated by lithium. Brain Res 2001;919:106–114. [PubMed: 11689167]

Klein PS, Melton DA. A molecular mechanism for the effect of lithium on development. Proc. Natl. Acad. Sci USA 1996;93:8455–8459. [PubMed: 8710892]

Koopman WJ, Verkaart S, Visch HJ, van Emst-de Vries S, Nijtmans LG, Smeitink JA, Willems PH. Human NADH:ubiquinone oxidoreductase deficiency: radical changes in mitochondrial morphology? Am. J. Physiol. Cell. Physiol 2007;293:22–29.

Ludolph AC, Seelig M, Ludolph A, Novitt P, Allen CN, Spencer PS, Sabri MI. 3-Nitropropionic acid decreases cellular energy levels and causes neuronal degeneration in cortical explants. Neurodegeneration 1992;1:155–161.

Milakovic T, Johnson GV. Mitochondrial respiration and ATP production are significantly impaired in striatal cells expressing mutant huntingtin. J. Biol. Chem 2005;280:30773–30782. [PubMed: 15983033]

Naerum L, Nørskov-Lauritsen L, Olesen PH. Scaffold hopping and optimization towards libraries of glycogen synthase kinase-3 inhibitors. Bioorg. Med. Chem. Lett 2002;12:1525–1528. [PubMed: 12031334]

Oliver FJ, de la Rubia G, Rolli V, Ruiz-Ruiz MC, de Murcia G, Murcia JM. Importance of poly(ADP-ribose) polymerase and its cleavage in apoptosis. Lesson from an uncleavable mutant. J. Biol. Chem 1998;273:33533–33539. [PubMed: 9837934]

Pap M, Cooper GM. Role of glycogen synthase kinase-3 in the phosphatidylinositol 3-Kinase/Akt cell survival pathway. J. Biol. Chem 1998;273:19929–19932. [PubMed: 9685326]

Parker PJ, Embi N, Caudwell FB, Cohen P. Glycogen synthase from rabbit skeletal muscle. State of phosphorylation of the seven phosphoserine residues *in vivo* in the presence and absence of adrenaline. Eur. J. Biochem 1982;124:47–55. [PubMed: 6211353]

Parker WD Jr, Boyson SJ, Parks JK. Abnormalities of the electron transport chain in idiopathic Parkinson's disease. Ann. Neurol 1989;26:719–723. [PubMed: 2557792]

Parker WD Jr, Parks JK, Swerdlow RH. Complex I deficiency in Parkinson's disease frontal cortex. Brain Res 2008;1189:215–218. [PubMed: 18061150]

Rao R, Hao CM, Breyer MD. Hypertonic stress activates glycogen synthase kinase 3β-mediated apoptosis of renal medullary interstitial cells, suppressing an NFκB-driven cyclooxygenase-2-dependent survival pathway. J. Biol. Chem 2004;279:3949–3955. [PubMed: 14607840]

Rizzuto R, Simpson AW, Brini M, Pozzan T. Rapid changes of mitochondrial Ca^{2+} revealed by specifically targeted recombinant aequorin. Nature 1992;358:325–327. [PubMed: 1322496]

Song L, De Sarno P, Jope RS. Central role of glycogen synthase kinase-3β in endoplasmic reticulum stress-induced caspase-3 activation. J. Biol. Chem 2002;277:44701–44708. [PubMed: 12228224]

Swerdlow RH, Parks JK, Miller SW, Tuttle JB, Trimmer PA, Sheehan JP, Bennett JP Jr, Davis RE, Parker WD Jr. Origin and functional consequences of the complex I defect in Parkinson's disease. Ann. Neurol 1996;40:663–671. [PubMed: 8871587]

Tewari M, Quan LT, O'Rourke K, Desnoyers S, Zeng Z, Beidler DR, Poirier GG, Salvesen GS, Dixit VM. Yama/CPP32β, a mammalian homolog of CED-3, is a CrmA-inhibitable protease that cleaves the death substrate poly(ADP-ribose) polymerase. Cell 1995;81:801–809. [PubMed: 7774019]

Wang W, Yang Y, Ying C, Li W, Ruan H, Zhu X, You Y, Han Y, Chen R, Wang Y, Li M. Inhibition of glycogen synthase kinase-3μ protects dopaminergic neurons from MPTP toxicity. Neuropharmacology 2007;52:1678–1684. [PubMed: 17517424]

Trimmer PA, Swerdlow RH, Parks JK, Keeney P, Bennett JP Jr, Miller SW, Davis RE, Parker WD Jr. Abnormal mitochondrial morphology in sporadic Parkinson's and Alzheimer's disease cybrid cell lines. Exp. Neurol 2000;162:37–50. [PubMed: 10716887]

Watcharasit P, Bijur GN, Zmijewski JW, Song L, Zmijewska A, Chen X, Johnson GV, Jope RS. Direct, activating interaction between glycogen synthase kinase-3β and p53 after DNA damage. Proc. Natl. Acad. Sci. USA 2002;99:7951–7955. [PubMed: 12048243]

Xavier IJ, Mercier PA, McLoughlin CM, Ali A, Woodgett JR, Ovsenek N. Glycogen synthase kinase 3β negatively regulates both DNA-binding and transcriptional activities of heat shock factor 1. J. Biol. Chem 2000;275:29147–29152. [PubMed: 10856293]

Yuan Y, Jin J, Yang B, Zhang W, Hu J, Zhang Y, Chen NH. Overexpressed α-synuclein regulated the nuclear factor-κB signal pathway. Cell. Mol. Neurobiol 2008;28:21–33. [PubMed: 17712623]

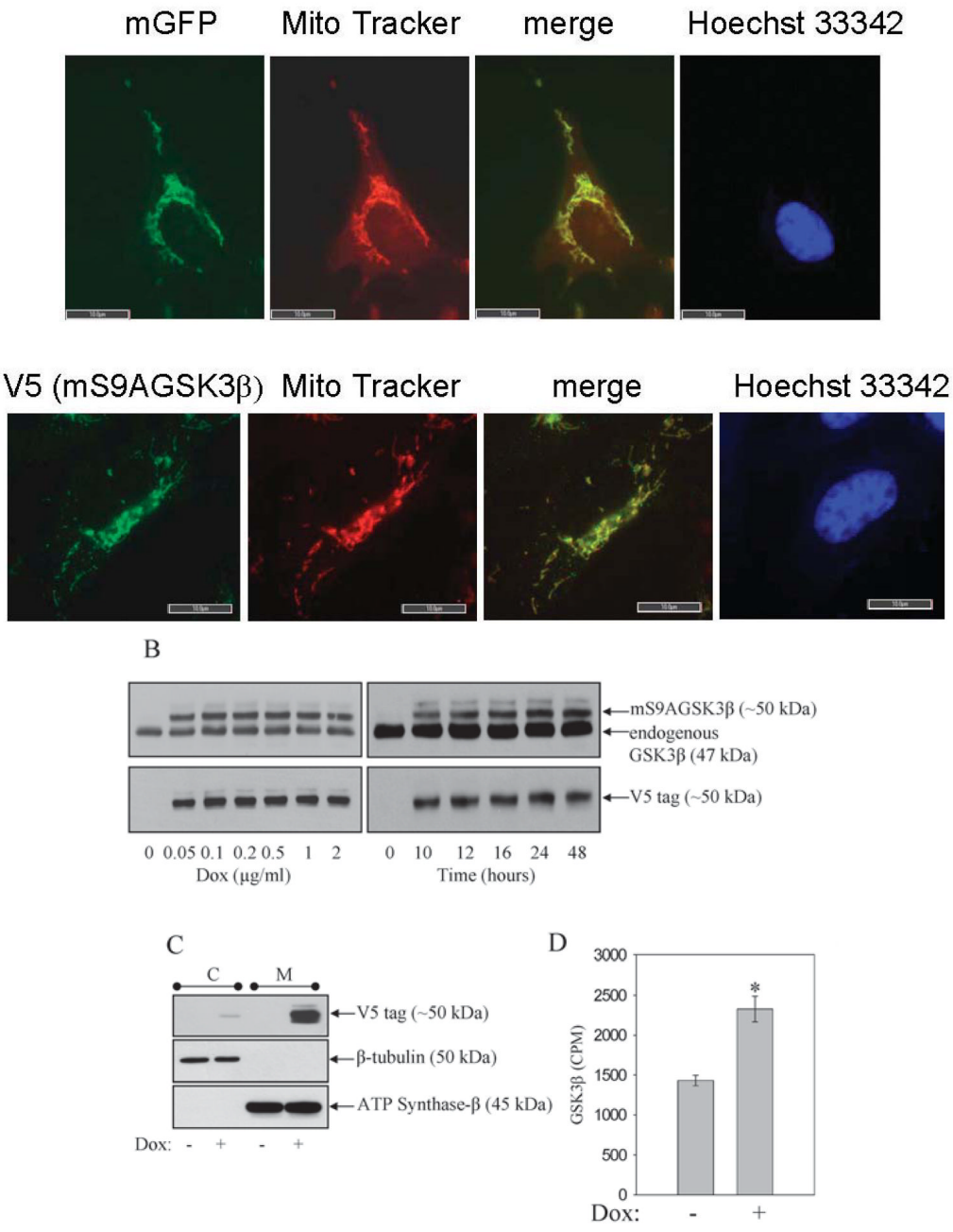

FIGURE 1. Expression of mitochondrial-targeted constitutively active GSK3β

A. Cells were plated on glass cover slips, treated with 1 μg/ml Dox for 24 h, and stained with MitoTracker (red-CMX-ROS). ***Top panels:*** cultured SH-SY5Y cells expressing mitochondrial-targeted GFP (mGFP), green GFP autofluorescence, and stained with Mito Tracker dye, red fluorescence. ***Bottom panels:*** V5-tagged mS9AGSK3β cells were immunofluorescently labeled with V5 antibody (green immunofluorescence) as described in "Methods", and stained with Mito Tracker dye. The green and red fluorescence images were merged (yellow) to reveal specific localization of mGFP and the V5-tagged mS9AGSK3β in mitochondria. Cells were stained with Hoechst 33342 to visualize the nucleus. The fluorescent staining was viewed and photographed using a fluorescence microscope. Size bar=10 μm, 100x

objective. **B.** Cells expressing mitochondrial-targeted constitutively active GSK3β (mS9AGSK3β) were treated with 0.05, 0.1, 0.2, 0.5, 1, or 2 μg/ml Dox for 24 h or 1 μg/ml Dox for 10, 12, 16, 24, or 48 h, and whole cell lysates were immunoblotted for total GSK3β or the V5 tag. **C.** mS9AGSK3β cells were treated with 1 μg/ml Dox, fractionated, and crude cytosolic and mitochondrial extracts were immunoblotted for V5 tag, β-tubulin, and ATP synthase-β. **D.** mS9AGSK3β cells were treated with 1 μg/ml Dox for 24 h and whole cell lysates were used to measure the activity of GSK3β as described in "Methods". Values are means ± S.E.M., n=3, *P <0.05, ANOVA.

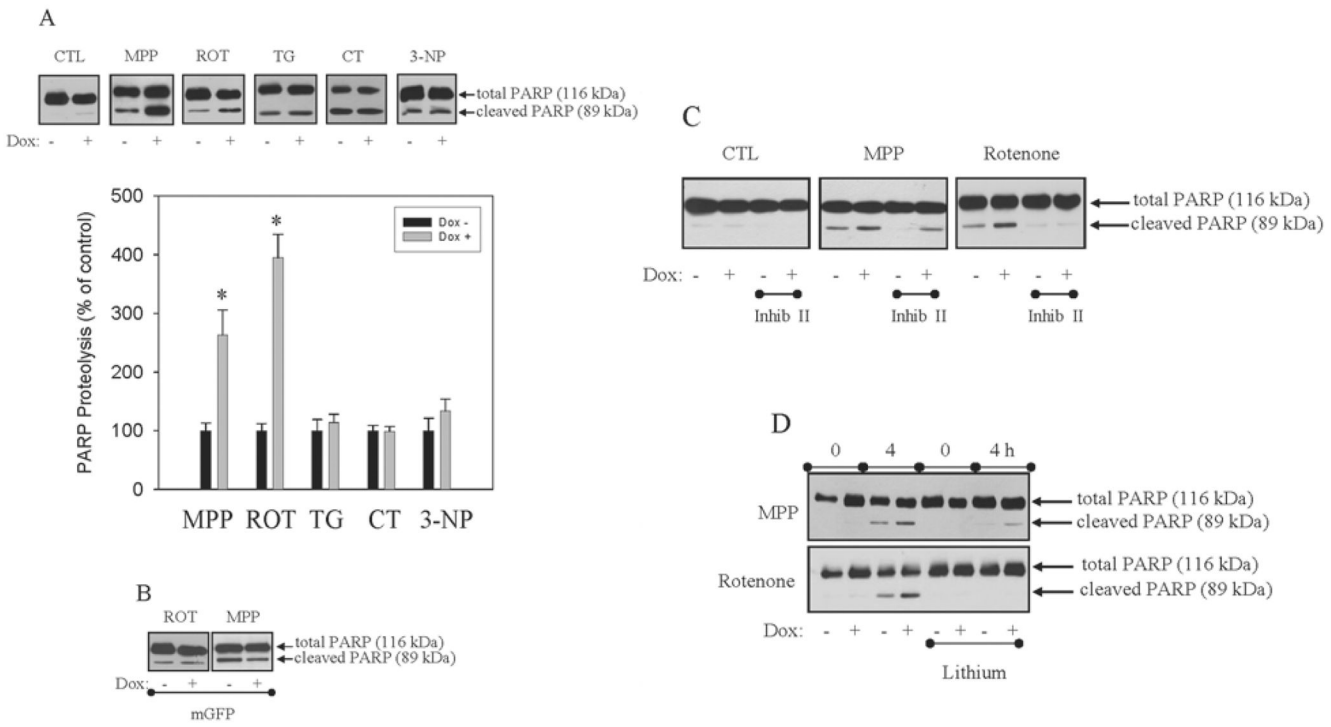

FIGURE 2. Unregulated mitochondrial GSK3β activity facilitates apoptosis induced by mitochondrial complex I inhibition, but not complex II inhibition, ER stress, nor genotoxic stress

A. mS9AGSK3β or mGFP cells were treated with Dox (1 μg/ml) for 24 h in serum-containing media and were transferred to serum free media containing Dox for 1 h prior to treatment with 5 mM 1-methyl-4-phenylpyridinium (MPP^+), 5 μM rotenone (ROT), 2 μM thapsigargin (TG), 1 μM camptothecin (CT), or 20 mM 3-nitropropionic acid (3-NP) for 4 h, and total cell lysates were immunoblotted for PARP. Quantitation of the proteolyzed PARP band for each sample is based on the percent of proteolyzed PARP from each sample's matched Dox- cells treated with the different apoptosis inducers. Values are means ± S.E.M., n=3, *P <0.05, ANOVA. **B.** Non-induced and induced mGFP cells were treated with 5 μM rotenone or 5 mM MPP^+ for 4 h, and total cell lysates were immunoblotted for PARP. mS9AGSK3β cells were treated with Dox (1 μg/ml) for 24 h in serum-containing media and were transferred to serum free media containing Dox for 1 h and (**C**) 5 μM 2-thio(3-iodobenzyl)-5-(pyridyl)-[1,3,4]-oxadiazole (inhib II) or (**D**) 20 mM lithium for 30 min prior to treatment with 5 mM MPP^+ or 5 μM rotenone for 4 h. PARP proteolysis was measured by Western blot analysis.

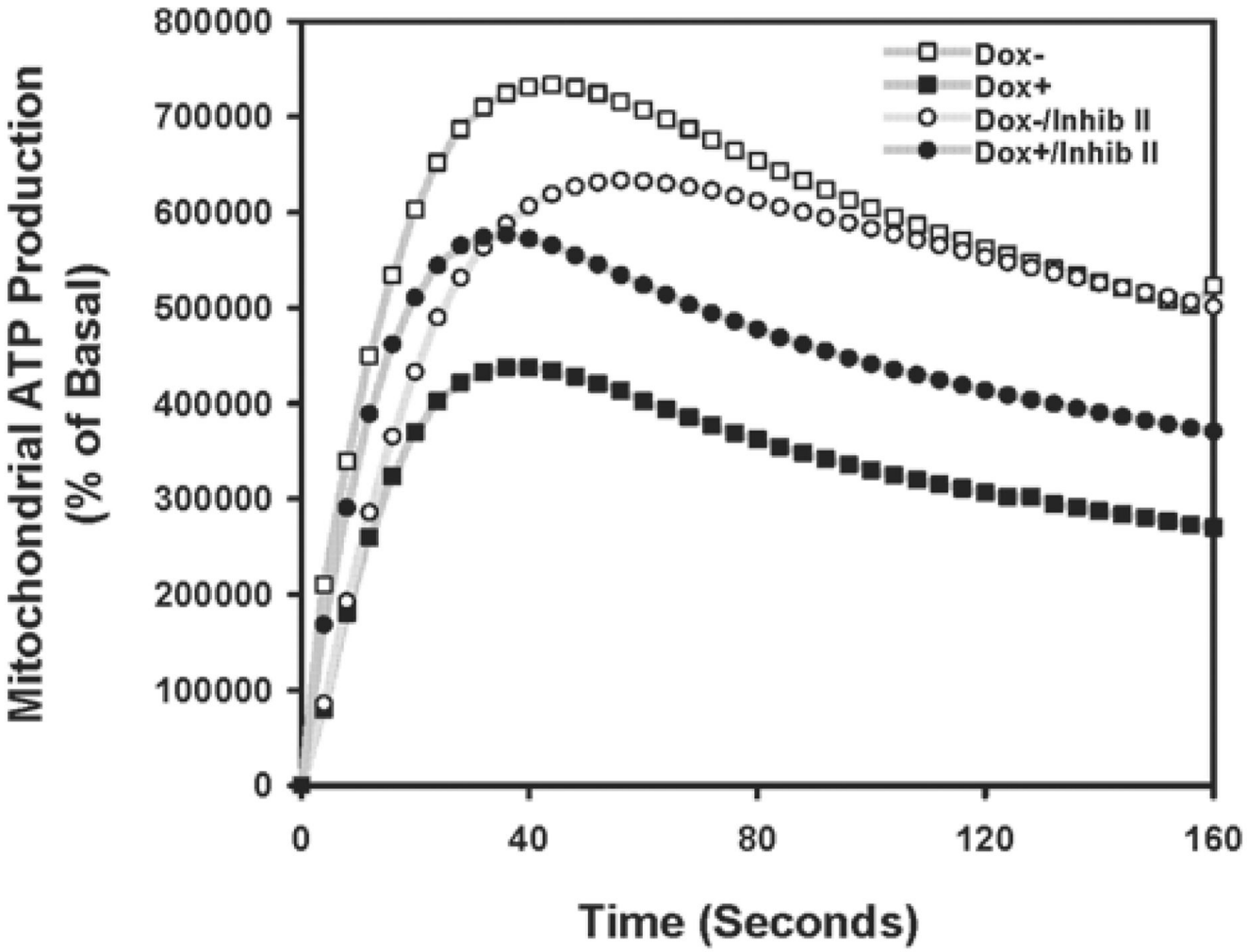

FIGURE 3. Unregulated mitochondrial GSK3β activity decreases mitochondrial ATP production

mS9AGSK3β cells were treated with Dox (1 μg/ml) for 24 h in serum media, and crude mitochondria were isolated from non-induced and induced cell cultures treated with and without 5 μM GSK3β inhibitor II for 4.5 h. ATP generation was measured as described in "Methods"

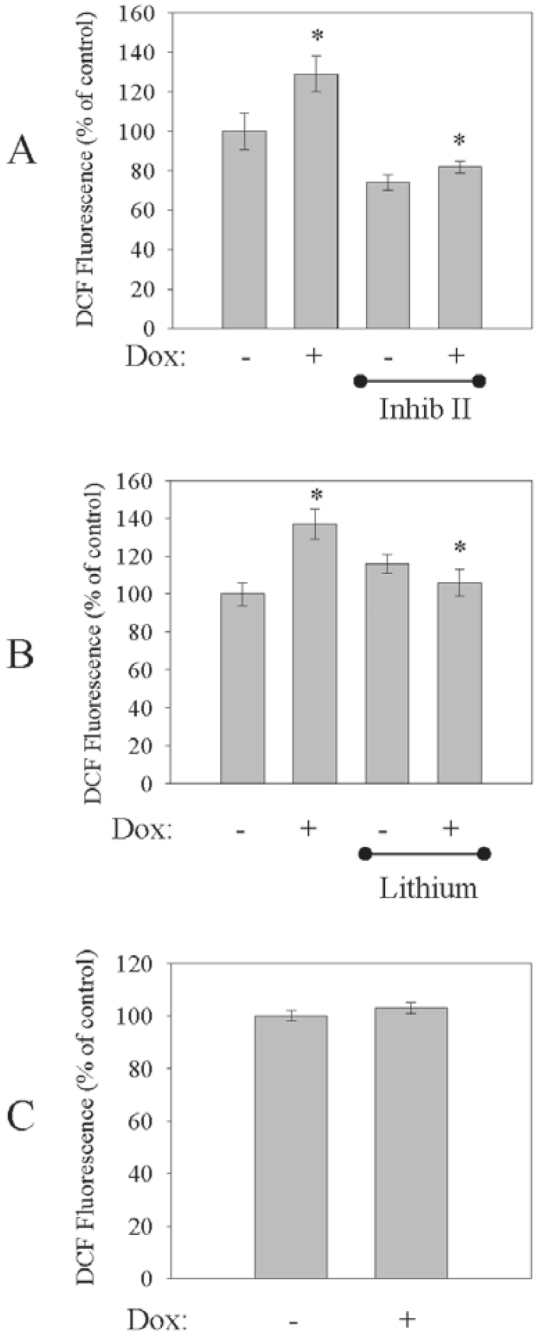

FIGURE 4. Unregulated mitochondrial GSK3β activity increases intracellular ROS production

mS9AGSK3β cells were treated with Dox for 24 h in serum media and were transferred to Dox-treated serum free media for 30 min prior to treatment with (**A, top**) 5 μM GSK3β inhibitor II (Inhib II) or (**B, middle**) 20 mM lithium for 4.5 h, and intracellular ROS production was measured as described in "Methods". **C, bottom**. SH-SY5Y/Tet-R control cells were treated with Dox (1 μg/ml) for 24 h in serum media and were transferred to Dox-treated serum-free media for 5 h, and intracellular ROS production was measured. Values are means ± S.E.M., n=3, *P <0.05, ANOVA.

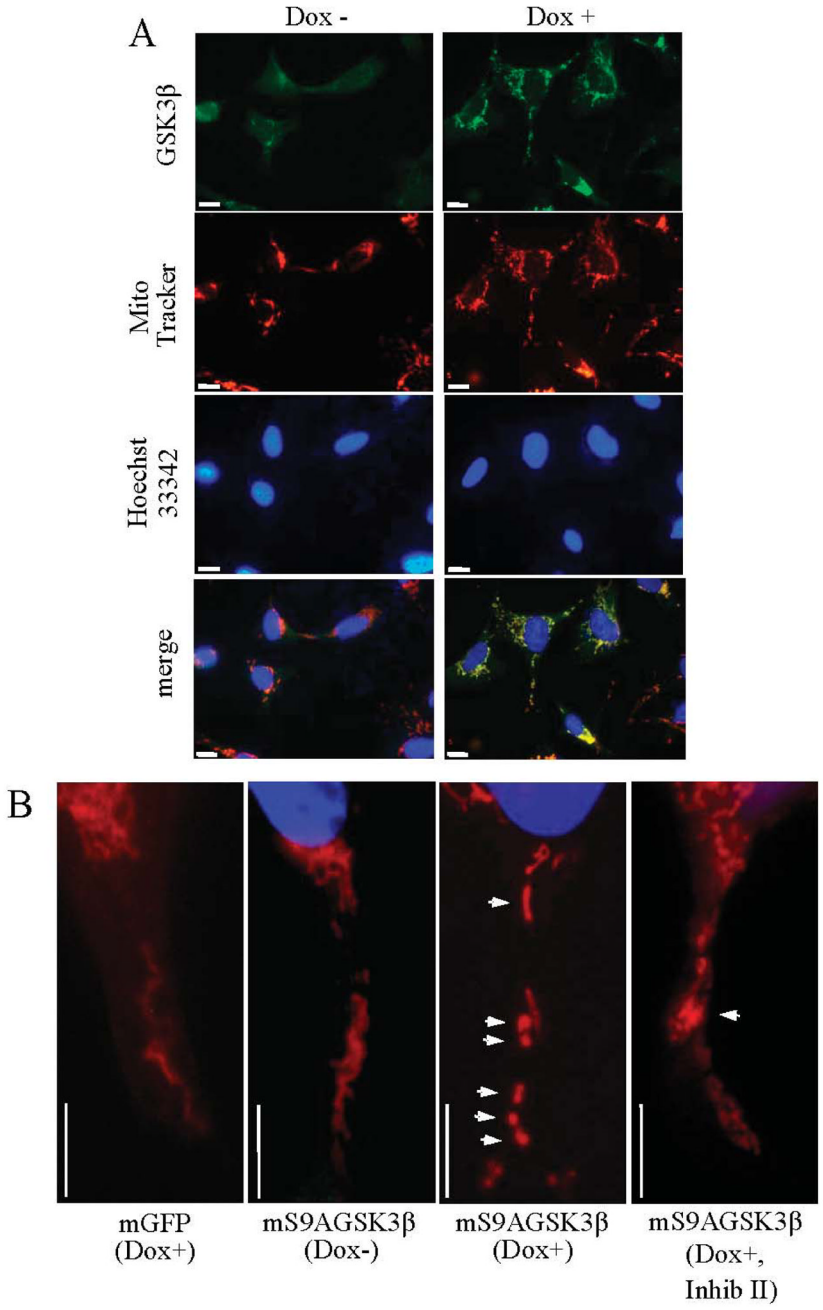

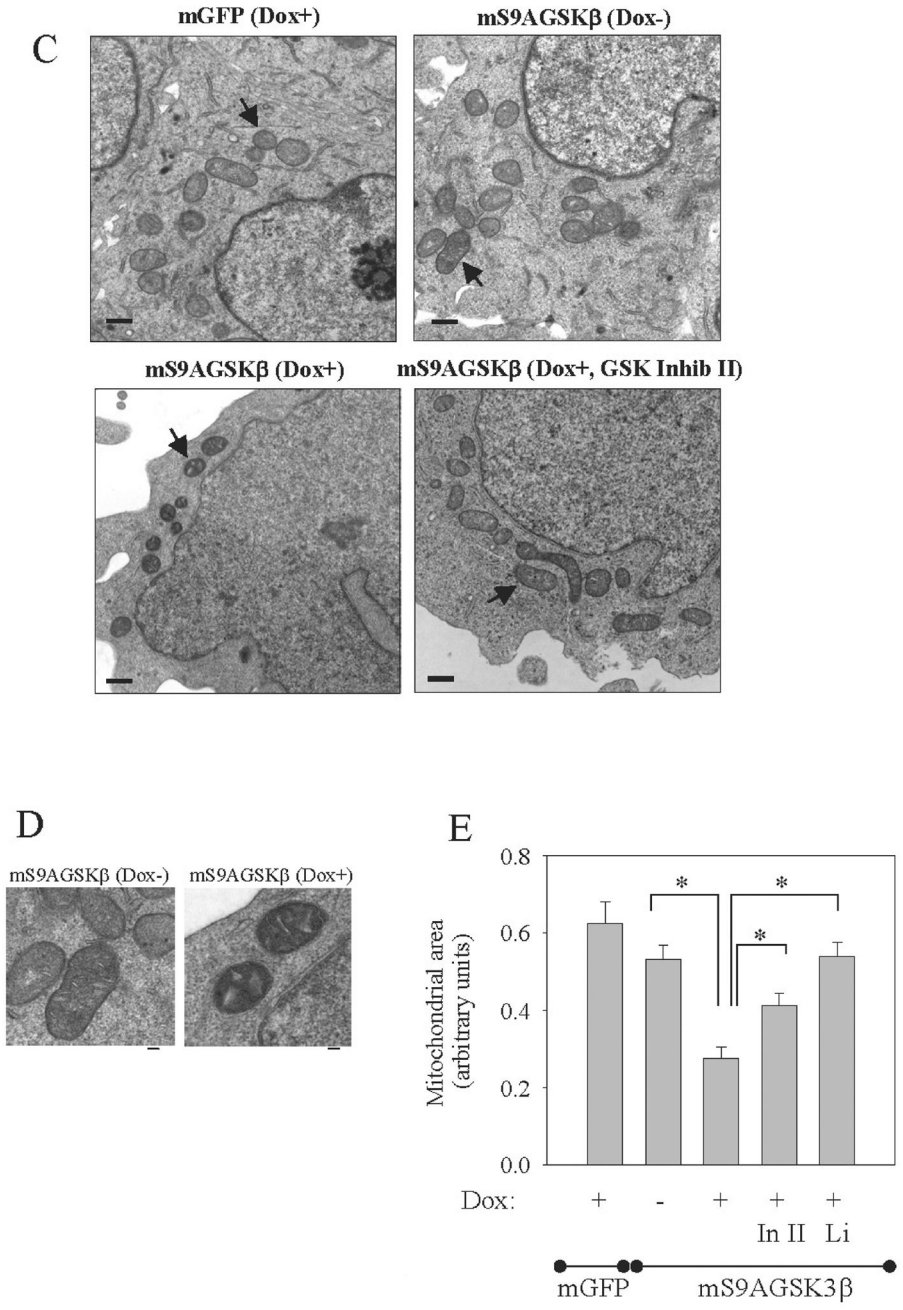

FIGURE 5. Unregulated mitochondrial GSK3β activity affects mitochondrial morphology

A. Doxycycline-induced (1 μg/ml, 24 h) expression of mS9AGSK3β reveals immunolocalization of the expressed protein in mitochondria and the altered mitochondrial morphology. Size bar=10 μm, 100x objective. **B.** Enhanced magnification of Mito Tracker-stained cells. Size bar=10 μm.

(**C–D**) mGFP and mS9AGSK3β cells were treated and prepared for transmission electron microscopy as described in the "Methods". The size bar in C = 500 nm and the size bar in D = 100 nm. **E**. Mitochondrial area was measured in pixels. "In II" is inhibitor II. Values are means ± S.E.M., 48 to 62 mitochondria per grid for each sample were counted, **P* <0.05, ANOVA.

Table I

Complex I activity. Isolated mitochondria were used to measure complex I activity as described in "Methods". The mS9AGSK3β or the mGFP cells were treated with Dox (1 μg/ml) for 24 h in serum-containing media and were transferred to serum free media containing Dox for 5 h or (mS9AGSK3ß) 30 min prior to treatment with 5 μM GSK3 inhibitor II for 4.5 h. The mitochondrial lysates from the non-induced and the induced mS9AGSK3β cells were incubated with 20 mM lithium for 30 min prior to measuring complex I activity. Values are represented as means ± S.E.M., n=3, *P <0.05, compared to the non-induced mS9AGSK3β cells.

Complex I Activity			
	Mean (% of control, Dox−)	**S.E.M**	**p<0.05 ANOVA**
mS9AGSK3β/Dox−	100	9	}*
mS9AGSK3β/Dox+	29	12	}*
mS9AGSK3β/Dox+/Inhib II	84	14	}*
mS9AGSK3β/Dox+/Li	65	8	}*
Controls			
mS9AGSK3β/Dox+/Inhib II	101	26	
mS9AGSK3β/Dox−/Li	97	21	
mGFP/Dox−	100	30	
mGFP/Dox+	160	90	